A simulation study of the optical Kerr effect in liquid water

ARTICLE *in* PHYSICAL CHEMISTRY CHEMICAL PHYSICS · MARCH 2005

Impact Factor: 4.49 · DOI: 10.1039/B417147K · Source: PubMed

3 AUTHORS:

Milton Taidi Sonoda
Universidade Federal do Triangulo Mineiro …
13 PUBLICATIONS **196** CITATIONS
SEE PROFILE

Sergio Vechi
Universität Heidelberg
8 PUBLICATIONS **104** CITATIONS
SEE PROFILE

Munir S Skaf
University of Campinas
85 PUBLICATIONS **1,732** CITATIONS
SEE PROFILE

RESEARCH PAPER

PCCP
www.rsc.org/pccp

A simulation study of the optical Kerr effect in liquid water

Milton T. Sonoda, Sérgio M. Vechi and Munir S. Skaf*

Instituto de Quumica, Universidade Estadual de Campinas, Cx. P. 6154, Campinas, SP, 13084-971, Brazil. E-mail: skaf@iqm.unicamp.br

Received 10th November 2004, Accepted 20th January 2005
First published as an Advance Article on the web 1st February 2005

A molecular dynamics simulation study is presented for the dynamics of the polarizability anisotropy of liquid water using the SPC/E model and a dipolar induction scheme that involves the intrinsic polarizability and first hyperpolarizability tensors obtained from *ab initio* quantum chemical calculations at the MP2/6-311++G(d,p) level. The time-correlation functions for the collective polarizability anisotropy, the optical Kerr effect response, and the frequency spectra are analyzed in terms of the intrinsic and induced polarizability contributions. At short times, the simulated Kerr nuclear response exhibits maxima near 15, 50 and 180 fs, followed by a diffusive tail which has been fitted by a bi-exponential with time constants *ca.* 0.4 and 2.5 ps. The short time features are in good agreement with available simulation and experimental results. The agreement with experiments is less satisfactory for the diffusive components. The main features of the frequency spectrum include a rotational-diffusion peak centered around 3 cm^{-1}, a collision-induced (hindered translations) band near 200 cm^{-1}, and a broad librational band at 450 cm^{-1}. The simulation results are in good agreement with experimental frequency spectra obtained from Kerr effect and related spectroscopies, but fail to reproduce the experimental band near 60 cm^{-1}.

1. Introduction

The intermolecular dynamics of liquid water has long been a subject of intense experimental and theoretical research.[1–5] Numerous experimental studies have been reported on the dynamics of liquid water in the last two or three decades using a variety of different techniques, including NMR,[6] microwave dielectric relaxation,[7] far-infrared,[8] Raman[9] and light scattering spectroscopies,[10] and small angle neutron scattering.[11] More recently, new experimental developments based on ultrafast laser techniques have made it possible to investigate intermolecular dynamical processes of water at much shorter timescales with substantially higher level of detail. Among these, terahertz spectroscopy[12] and nonlinear optical methods such as Raman echo[13] and optical Kerr effect[14,15] spectroscopies stand out for providing remarkably valuable information directly in the time domain.

Parallel to these developments, advances in molecular dynamics (MD) computer simulations have markedly enriched our views on the dynamics of water, both at ambient and nonambient conditions of temperature and pressure.[1] A variety of MD simulation studies have been performed on liquid water focusing on different aspects of its dynamics. In particular, detailed simulation analyses have been reported for dielectric relaxation, depolarized Raman or light scattering, time resolved fluorescence spectroscopy,[5] and nonlinear optical Kerr response for bulk phases,[16,17] as well as second harmonic generation and vibrational sum frequency[18] signals for studying interfacial aqueous systems more specifically. MD simulations have been carried out for the Kerr effect by Saito and Ohmine[16] on the TIPS2 potential at room temperature and by Bursulaya and Kim[17] on a mixed quantum-classical model for the electronic polarizability. The depolarized Raman spectrum of TIP4P water was studied at several temperatures as well.[19] Very recently, we have reported MD simulations of the Kerr response of binary dimethylsulfoxide–water mixtures, in which we investigate the effects of the H-bonding between water and DMSO on the mixtures' Kerr response.[20]

In this paper, we report MD simulations results for the polarizability anisotropy relaxation of liquid water at ambient conditions. Our goal is to examine, from a microscopic perspective, the characteristics of the intermolecular dynamics that are directly probed by depolarized Raman scattering or optical Kerr effect (OKE) spectroscopy.[14] Here we use Torii's extended dipole–induced-dipole model[21] for the collective polarizability and keep separate the contributions from the intrinsic and induced polarizabilities in order to identify the molecular origin of the different features that characterize water's OKE response.

In Section 2 we summarize the main theoretical relationships involved in the calculation of the OKE signals from the simulations and describe the computational details. Results and discussions appear in Section 3. Our concluding remarks are presented in Section 4.

2. Theory and computational details

2.1. Theoretical background

The relevant dynamical variable for the spectroscopic properties of interest is the collective electronic polarizability tensor of the system, $\boldsymbol{\Pi}$:[22,23]

$$\boldsymbol{\Pi} = \sum_{i}^{N} \alpha_i = \boldsymbol{\Pi}^{\mathrm{M}} + \boldsymbol{\Pi}^{\mathrm{I}}, \qquad (1)$$

where the total polarizability has been separated into intrinsic (molecular), $\boldsymbol{\Pi}^{\mathrm{M}}$, and induced, $\boldsymbol{\Pi}^{\mathrm{I}}$ contributions. The intrinsic part is the sum of unperturbed, gas phase molecular polarizabilities,

$$\boldsymbol{\Pi}^{\mathrm{M}} = \sum_{i}^{N} \alpha_i^{\mathrm{M}}, \qquad (2)$$

while the induced part comprises polarizability enhancements due to the intermolecular interactions. In this work, the dynamical modulation of the polarizabilities arises from a

DOI: 10.1039/b417147k

center-to-center dipolar coupling between molecules:

$$\boldsymbol{\Pi}^{\mathrm{I}} = \sum_{i}^{N} \sum_{j \neq i} \left(\boldsymbol{\alpha}_i^{\mathrm{M}} \; \boldsymbol{T}_{ij} \; \boldsymbol{\alpha}_j + \boldsymbol{\beta}_i^{\mathrm{M}} \; \boldsymbol{T}_{ij} \; \boldsymbol{\mu}_j \right). \tag{3}$$

The enhanced polarizability tensor and dipole vector of the molecules are obtained by iteratively solving the equations:

$$\boldsymbol{\alpha}_i = \boldsymbol{\alpha}_i^{\mathrm{M}} + \sum_{j \neq i} \boldsymbol{\alpha}_i^{\mathrm{M}} \; \boldsymbol{T}_{ij} \; \boldsymbol{\alpha}_j \tag{4}$$

$$\boldsymbol{\mu}_i = \boldsymbol{\mu}_i^{\mathrm{M}} + \sum_{j \neq i} \boldsymbol{\alpha}_i^{\mathrm{M}} \; \boldsymbol{T}_{ij} \; \boldsymbol{\mu}_j, \tag{5}$$

where $\boldsymbol{\mu}_i^{\mathrm{M}}$ and $\boldsymbol{\beta}_i^{\mathrm{M}}$ are the gas phase dipole and hyperpolarizability of molecule i, respectively, and $\boldsymbol{T}_{ij} = \nabla_i \nabla_j \mid \boldsymbol{r}_i - \boldsymbol{r}_j \mid^{-1}$ is the dipole tensor between molecules i and j. All vectors and tensors are expressed in the lab frame. This enhancement mechanism, named extended dipole–induced-dipole (XDID),[21] includes contributions from the first hyperpolarizability of the molecule and has been used in recent simulations of depolarized Raman spectrum and OKE responses of formamide and *N*-methylformamide,[21] and DMSO/water mixtures.[20] By neglecting the "$\beta T \mu$" term, one recovers the usual dipole–induced-dipole (DID) mechanism.[24]

The dynamics of interest here is given by time-correlation function (TCF) of the off-diagonal elements of the collective polarizability tensor:

$$\Psi(t) = \langle \boldsymbol{\Pi}_{xz}(t) \; \boldsymbol{\Pi}_{xz}(0) \rangle / \; (N\gamma^2)/15) \tag{6}$$

where $\gamma^2 = \frac{1}{2}[(\alpha_1 - \alpha_2)^2 + (\alpha_1 - \alpha_3)^2 + (\alpha_2 - \alpha_3)^2]$ is the square of the ideal polarizability anisotropy, with α_j as the principal polarizability components. To improve statistics, $\Psi(t)$ is computed from all the independent TCFs of off-diagonal elements (xy, xz and yz).

2.2. Models and simulations

The intrinsic molecular polarizability and first hyperpolarizability tensors were obtained from *ab initio* quantum chemical calculations with electronic correlation taken into account at the MP2 level and basis set 6-311++G(d,p) using the Gaussian98 program package.[25] The nonzero elements of the α^{M} and β^{M} tensors for water are collected in Table 1. Simulations were also performed using α^{M} and β^{M} tensors computed at the MP3/6-31+G(2df,p) level, yielding practically identical results for the spectroscopic quantities of interest. The molecular coordinate axes are defined with the y-axis normal to the molecular plane and the z-axis along the dipole. The polarizability and first hyperpolarizability tensors obtained from our calculations are consistent with the quantum calculations of Gubskaya and Kusalik.[26] There are, however, appreciable differences between our β^{M} tensor (including the sign of some components) and the results obtained from higher level coupled-cluster calculations.[27,28] The effects of different β^{M} tensors on the OKE response was not fully investigated, but are expected to be small since the DID contribution is markedly predominant.

Table 1 Nonzero components of the molecular polarizability and first hyperpolarizability tensor obtained from electronic structure computations at the MP2/6–311++G(d,p) level. The components of α^{M} and β^{M} are given in units of Å^3 and Å$^5/e$, respectively

	$\alpha_{xx}{}^{\mathrm{M}}$	$\alpha_{xy}{}^{\mathrm{M}}$	$\alpha_{yy}{}^{\mathrm{M}}$	$\alpha_{zz}{}^{\mathrm{M}}$
Water[a]	1.04	0	1.00	1.17

	$\beta_{xxx}{}^{\mathrm{M}}$	$\beta_{xxz}{}^{\mathrm{M}}$	$\beta_{xyy}{}^{\mathrm{M}}$	$\beta_{yyz}{}^{\mathrm{M}}$	$\beta_{zzz}{}^{\mathrm{M}}$
Water[a]	0.80	−0.19	0.06	0.05	0.86

[a] The z- and y-directions for water are along the C_{2v} symmetry axis and normal to the molecular plane, respectively. The β_{yzz} components is smaller than 0.05 Å$^5/e$ and the remainders are zero.

The MD trajectories were generated using the well-known SPC/E potential for water,[29] which treats the molecules as nonpolarizable, rigid bodies interacting *via* a pairwise sum of site-site potentials involving standard (12–6) Lennard-Jones plus Coulombic terms. The simulations were performed in the *NVE* ensemble with a total of $N = 500$ molecules placed in periodically replicated cubic boxes dimensioned to reproduce the experimental density at ambient conditions (0.997 g cm^{-3}).

Lennard-Jones forces were cut-off at half the box length and Coulomb forces were treated *via* Ewald sums with conducting boundaries.[30] The equations of motion were integrated with SHAKE[31] and leap-frog algorithms[32] with a timestep of 3 fs. Total energy is conserved within 0.2% during unperturbed 12 ps runs. Approximately 200 of such runs, separated by occasional intervals for velocity rescaling, were used to compute the quantities of interest.

3. Results and discussion

According to eqn. (1)–(6), $\Psi(t)$ has contributions from molecular and induced autocorrelations plus the cross-correlation between molecular and induced polarizabilities:

$$\Psi(t) = \Psi^{\mathrm{MM}}(t) + \Psi^{\mathrm{II}}(t) + \Psi^{\mathrm{MI}}(t), \tag{7}$$

with

$$\Psi^{\mathrm{MM}}(t) = \langle \boldsymbol{\Pi}_{xz}{}^{\mathrm{M}}(t) \boldsymbol{\Pi}_{xz}{}^{\mathrm{M}}(0) \rangle / (N\gamma^2/15); \quad \Psi^{\mathrm{II}}(t) = \langle \boldsymbol{\Pi}_{xz}{}^{\mathrm{I}}(t) \boldsymbol{\Pi}_{xz}{}^{\mathrm{I}}(0) \rangle / (N\gamma^2/15) \tag{8}$$

$$\Psi^{\mathrm{MI}}(t) = (\langle \boldsymbol{\Pi}_{xz}{}^{\mathrm{M}}(t) \boldsymbol{\Pi}_{xz}{}^{\mathrm{I}}(0) \rangle + \langle \boldsymbol{\Pi}_{xz}{}^{\mathrm{I}}(t) \boldsymbol{\Pi}_{xz}{}^{\mathrm{M}}(0) \rangle) / (N\gamma^2/15) \tag{9}$$

Being an intrinsically collective quantity, $\Psi(t)$ may be a slowly converging property. To assure that the simulations are long enough to yield converged anisotropy correlations, we have computed the cumulative averages for $\Psi^{\mathrm{MM}}(0)$, $\Psi^{\mathrm{II}}(0)$, and $\Psi^{\mathrm{MI}}(0)$ as functions of the simulation time. The results are shown in Fig. 1, which clearly indicate that convergence has been reached. The estimated relative errors are less than 5%. The

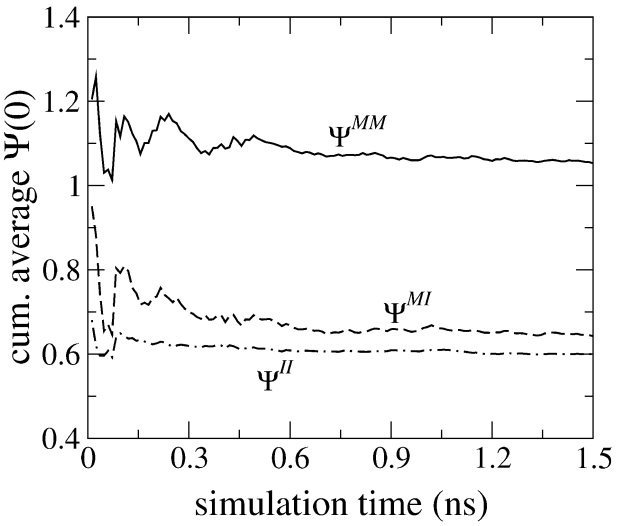

Fig. 1 Cumulative average of the static fluctuations of the collective polarizability anisotropy for SPC/E water *versus* simulation time. The intrinsic molecular (MM) fluctuation is shown by a solid line, the induced (II) and cross-correlation (MI) contributions are shown by dashed and dashed-dotted lines, respectively.

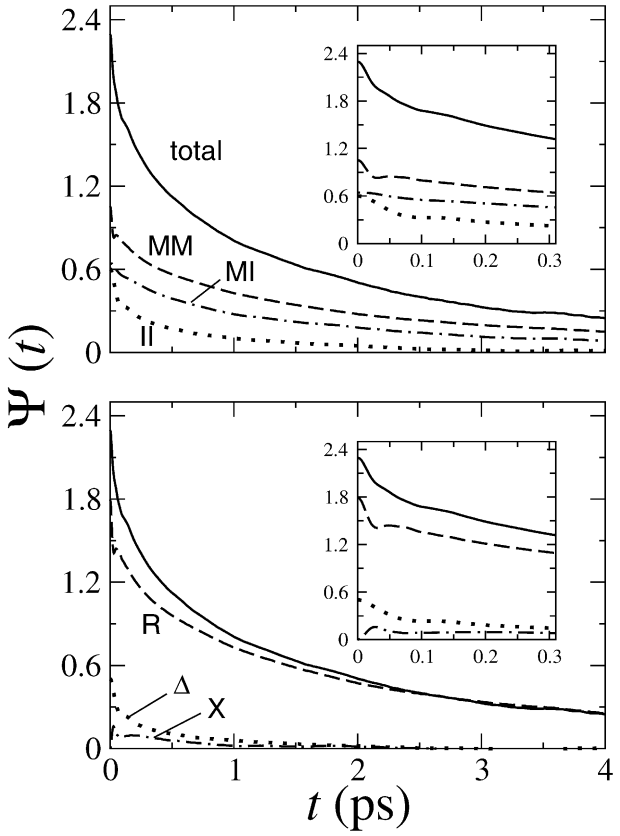

Fig. 2 Total collective polarizability anisotropy relaxation (solid line), intrinsic molecular contributions (MM; dashed line), induced polarizability auto-correlation (II; dotted line), and cross-correlation (MI; dashed-dotted line). The insert shows features of the short-time dynamics. The lower panel shows the total TCF and the separate contributions in terms of projected variables. Solid line: $\Psi(t)$; dashed line: $\Psi^{R}(t)$; Dotted line: $\Psi^{\Delta}(t)$; dashed-dotted line: $\Psi^{X}(t)$.

total static correlation, $\Psi(0) = 2.33$, is substantially higher than the uncorrelated value of $\Psi^{ideal} = 1.0$ because of the intrinsic structure of liquid water. The molecular and induced autocorrelations at $t = 0$ contribute nearly 46 and 26%, respectively, while the cross-correlation represents the remaining 28%.

Fig. 2, upper panel, shows the relaxation of the total anisotropy, $\Psi(t)$ (solid line) and its separate contributions, Ψ^{MM}, Ψ^{II} and Ψ^{MI}. The insert shows details of the initial stages of the relaxation in which librational oscillations are evident. After the librational transient, the relaxation rates of all three components are similar, which suggests that the induced polarizabilities tend to follow the reorientational dynamics of the molecules. The post-librational decay is well-described by a bi-exponential relaxation, $a_1\exp(-t/\tau_1) + a_2 \exp(-t/\tau_2)$, in the time interval 0.2–6.0 ps. Our best fitting parameters are given in Table 2. The characteristic decay times for the total $\Psi(t)$, 0.37 and 2.46 ps, are roughly comparable to the experimental values reported by Castner and co-workers (0.50 and 1.19 ps).[33] In this time interval, $\Psi(t)$ can be equally well fitted by a stretched exponential function, $a_0 \exp[-(t/\tau_0)^{\beta}]$, with $\tau_0 = 1.01$ ps and $\beta = 0.59$. Very recent experimental OKE data yield $\tau_0 = 0.35$ ps and $\beta = 0.58$ for water at 294 K.[34] The rotational-diffusion relaxation of the simulated OKE signal is therefore slower than the experimentally observed dynamics. How much of the total TCF is due to reorientational processes can be determined by means of the projection scheme used to analyze the dielectric relaxation of polar-polarizable fluids.[35] Namely, the collective polarizability tensor components are separated into "local-field" and "collision-induced" portions according to:[35,36]

$$\boldsymbol{\Pi}_{xz}{}^{I}(t) = G\boldsymbol{\Pi}_{xz}{}^{M}(t) + \Delta\boldsymbol{\Pi}_{xz}(t), \qquad (10)$$

Table 2 Bi-exponential, $a_1 \exp(-t/\tau_1) + a_2 \exp(-t/\tau_2)$, fits to the polarizability anisotropy TCF in the time intervals 0.2–6.0 ps

	a_1	τ_1/ps	a_2	τ_2/ps
$\Psi(t)$	0.76	0.37	1.14	2.46
$\Psi^{MM}(t)$	0.30	0.45	0.56	2.90
$\Psi^{II}(t)$	0.24	0.16	0.25	1.16
$\Psi^{MI}(t)$	0.23	0.33	0.42	2.36

where

$$G = \langle \boldsymbol{\Pi}_{xz}{}^{M}(0)\boldsymbol{\Pi}_{xz}{}^{I}(0)\rangle / \langle |\boldsymbol{\Pi}_{xz}{}^{M}(0)|^2\rangle \qquad (11)$$

is the static projection of the induced polarizability over the molecular polarizability. From the simulations we obtain $G = 0.30$. The quantity

$$\Delta\boldsymbol{\Pi}_{xz}(t) = \boldsymbol{\Pi}_{xz}{}^{I}(t) - G\boldsymbol{\Pi}_{xz}{}^{M}(t) \qquad (12)$$

represents the time-dependent fluctuations of the induced polarizability around the intrinsic counterpart renormalized by the induced effects. Thus, the projection allows the separation of the translational contributions (collision-induced) from the reorientational components of the polarizability anisotropy relaxation.

In terms of projected variables, the total TCF can be separated into a purely "reorientational" (R), a "collision-induced" contribution (Δ), and their cross correlation (X):

$$\Psi(t) = \Psi^{R}(t) + \Psi^{X}(t) + \Psi^{\Delta}(t), \qquad (13)$$

with

$$\Psi^{R}(t) = (1 + G)^2\Psi^{MM}(t) \qquad (14)$$

and

$$\Psi^{X}(t) = 2(1 + G)\langle \Delta\boldsymbol{\Pi}_{xz}(t)\boldsymbol{\Pi}_{xz}{}^{M}(0)\rangle/(N\gamma^2/15) \qquad (15)$$

$$\Psi^{\Delta}(t) = \langle \Delta\boldsymbol{\Pi}_{xz}(t)\Delta\boldsymbol{\Pi}_{xz}(0)\rangle/(N\gamma^2/15). \qquad (16)$$

The lower panel of Fig. 2 shows the total TCF (solid line) and the projected contributions. The data clearly shows that the renormalized intrinsic contribution $\Psi^{R}(t)$ (dashed line) predominates over the other components. Although the magnitude of the collision-induced contribution Ψ^{Δ} at early times is less than a third of the reorientational counterpart, there are some important features due to the translational dynamics that will appear in the OKE signal itself, as discussed below. The results depicted in Fig. 2, lower panel, also show that the simulated anisotropy relaxation in the rotational-diffusion regime ($t > 2$ ps), is essentially given by the reorientational component $\Psi^{R}(t)$.

The optically heterodyne-detected OKE signal in the time domain provides valuable information about the intermolecular dynamics through the nuclear response function, $R^{nuc}(t)$, which is experimentally obtained from the raw OKE transients after removal of the instantaneous electronic response and deconvolution from the instrument function.[14,24,37] Simply put, $R^{nuc}(t)$ is related to the time derivative of the anisotropy polarizability TCF through:

$$R^{nuc}(t) = -\frac{1}{k_B T}\frac{\partial\Psi(t)}{\partial t}. \qquad (17)$$

Fig. 3 shows the total nuclear response function (thick solid line) and the separate contributions from $\partial\Psi^{MM}(t)/\partial t$, $\partial\Psi^{II}(t)/\partial t$, and $\partial\Psi^{MI}(t)/\partial t$. The cross-correlation between molecular and induced polarizabilities makes a negligible contribution to $R^{nuc}(t)$ because Ψ^{MI} is a slowly varying function of time (*cf.* Fig. 2). The nuclear response function and its R_{MM} component present a rapid initial rise to their maxima within the first 15 fs, followed by a brief period of oscillatory decay, which subsequently merges into a smooth relaxation. Like the case of acetonitrile[38] and polar protic solvents,[17,36,39] the simulated

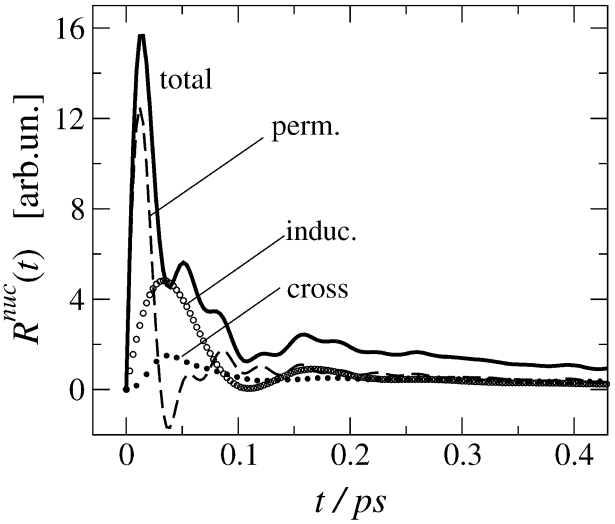

Fig. 3 OKE nuclear response for SPC/E water within the XDID scheme. Total, molecular, induced and cross-correlation contributions are as indicated.

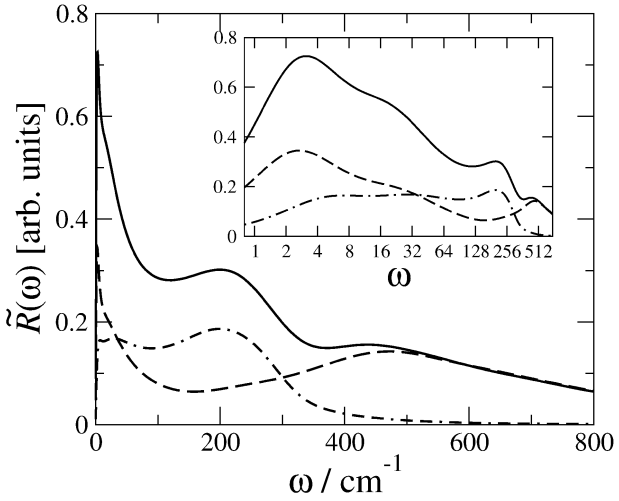

Fig. 4 OKE frequency spectra for SPC/E water within the XDID scheme. Solid, dashed-dotted, and dashed lines correspond to total, induced, and cross-correlation spectra. The insert depicts the spectra *versus* ω on a logarithmic scale, which shows the low-frequency band in greater detail.

$R^{\mathrm{nuc}}(t)$ function shows prominent oscillatory features associated to fast hindered reorientational motions because of water's small moments of inertia and strong intermolecular association. The behavior of the simulated OKE nuclear response presented here lies somewhere in-between the nuclear responses reported by Bursulaya and Kim[17] obtained from simulations with the TAB/10D polarizable water potential and a fixed, nonfluctuating (NF) molecular polarizability model. Specifically, our $R^{\mathrm{nuc}}(t)$ shows less pronounced oscillations in the time interval of Fig. 3 than does TAB/10D water, but is noticeably more oscillatory than the response from the NF model.[17] The features near 12–20 and 150 fs from both TAB/10D and NF simulations, are also present here. The structure near 50 fs is due to librational motions[40] and has been observed with the TAB/10D potential but not with the NF model.[17] These results imply that important dynamical fluctuations of water polarizability, particularly the effects of the solvent nonlinear electronic response, are only partially accounted for by our simulations through the "$\beta T\mu$" term, with quantitative consequences to the OKE transients and also to the frequency spectra, discussed below. Overall, there is reasonable agreement with the experimental nuclear response reported by Castner *et al.*,[15] which shows peaks at *ca.* 20, 57 and 197 fs. Interestingly, the simulation results shown in Fig. 3 indicates that the peak between 150–200 fs is mainly due to collision-induced dynamics, which corroborates the experimental interpretation of this feature in terms of hindered translational modes within the cage of neighbors.

Further comparison with available experimental data can be made in terms of the frequency spectra. The spectrum of interest here is provided by the imaginary part of the Fourier transform of the nuclear response according to:[17,37]

$$\tilde{R}(\omega) = 2\,\frac{1-e^{-\beta\hbar\omega}}{1+e^{-\beta\hbar\omega}}\int_0^\infty \sin(\omega t)R^{\mathrm{nuc}}(t)\,\mathrm{d}t\,, \qquad (18)$$

where $1/\beta = k_{\mathrm{B}}T$. The detailed balance desymmetrization factor $2/(1+e^{-\beta\hbar\omega})$, which accounts for quantum corrections to the classical spectrum, has been explicitly indicated.[17,41] This relationship indicates that depolarized Raman or light scattering and OKE spectra are closely related quantities.[37] The long-time portion of the $R^{\mathrm{nuc}}(t)$ response, is *ca.* $-\partial[a_1\exp(-t/\tau_1) + a_2\exp(-t/\tau_2)]/\partial t$ was used in order to improve the accuracy of the numerical Fourier transforms. Results for $\tilde{R}(\omega)$ are shown in Fig. 4. The spectrum of the total nuclear response (solid line) presents peaks at different frequencies corresponding to the intricate motions of water.

The slow rotational-diffusion dynamics is mainly characterized by a central band near 3 cm^{-1} and a shoulder between 20 and 30 cm^{-1} (Fig. 4, insert). The band shape in this frequency region is given essentially by the molecular (MM) polarizability auto-correlations. The rotational-diffusion relaxation obtained from our SPC/E-based simulations is slower than that reported for the TAB/10D model, which has a maximum in the reorientational band near 8 cm^{-1}.[17] For higher frequencies, two main peaks are identified in the total spectrum at *ca.* 230 and 500 cm^{-1}, which are due to induced (II) and molecular (MM) polarizability auto-correlations, respectively. The simulated spectrum is qualitatively compared with the experimental[15] analyses from different groups, which ascribe the measured broad band in the range 400–800 cm^{-1} to hindered reorientational motions (librations) about the different molecular axes, and the peaks at *ca.* 60 and 170 cm^{-1} to collision-induced effects from hindered translational motions associated with the stretching and bending of hydrogen bonds.[15,16] The experimentally observed feature near 60 cm^{-1} is not resolved in our simulations because the intrisinc polarizability (MM) contribution picks up intensity as ω falls below *ca.* 60 cm^{-1}. This suggests that the intrinsic polarizability tensor used in the simulations may overestimate the anisotropy of water.

4. Concluding remarks

In this work we report an MD simulation study of the polarizability anisotropy relaxation of SPC/E water, focusing on the Kerr nuclear responses in the time- and frequency-domains. The simulations require a model for the collective polarizability which has been described by a sum of individual molecular polarizabilities obtained from *ab initio* electronic structure calculations with a dynamical modulation given by a dipolar coupling. Some degree of nonlinear electronic response is incorporated through fixed (intrinsic) values of molecular hyperpolarizability tensors. We have analyzed the relaxation of the polarizability anisotropy in terms of the dynamics of intrinsic and induced polarizabilities and interpreted the OKE response and its spectrum in the light of the different contributions. Our results are compared with available experimental data and previous simulation results.

Acknowledgements

We gratefully acknowledge financial support from the Brazilian agencies FAPESP (Grants 01/09374-3 and 03/09163-4) and CNPq, and CAPES for a Graduate Fellowship to M.T.S.

References

1 Over the years, there have appeared numerous excellent reviews on water and aqueous systems. Refs. 2–5 serve as a starting point to the literature. The reader may also see the recent Special Issues: *Chem. Phys*., **258** (2000) and *Braz. J. Phys*., **34** (2004).
2 (*a*) F. H. Stillinger, *Adv. Chem. Phys*., 1975, **31**, 1; (*b*) F. H. Stillinger, *Science*, 1980, **209**, 451.
3 P. J. Rossky, *Annu. Rev. Phys. Chem*., 1985, **36**, 321.
4 I. Ohmine and H. Tanaka, *Chem. Rev*., 1993, **7**, 2545.
5 B. M. Ladanyi and M. S. Skaf, *Annu. Rev. Phys. Chem*., 1993, **44**, 335.
6 J. Jonas, T. DeFries and D. J. Wilbur, *J. Chem. Phys*., 1981, **65**, 581.
7 U. Kaatze and V. Uhlendorf, *Z. Phys. Chem., Neue Folge*, 1981, **126**, 151.
8 (*a*) M. N. Afsar and J. B. Hasted, *J. Opt. Soc. Am*., 1977, **67**, 902; (*b*) J. B. Hasted, S. K. Husain, F. A. M. Frescura and J. R. Birch, *Chem. Phys. Lett*., 1985, **118**, 622; (*c*) A. N. Rusk, D. Williams and M. R. Querry, *J. Opt. Soc. Am*., 1971, **61**, 895.
9 (*a*) A. de Santis, M. Sampoli, V. Mazzacurati and M. A. Ricci, *Chem. Phys. Lett*., 1987, **133**, 381; (*b*) A. de Santis, R. Frattini, M. Sampoli, V. Mazzacurati, M. Nardone, M. A. Ricci and G. Ruocco, *Mol. Phys*., 1987, **61**, 1199; (*c*) K. Mizoguchi, Y. Hori and Y. Tominaga, *J. Chem. Phys*., 1992, **97**, 1961.
10 C. J. Montrose, J. A. Bucaro, J. Marshall-Coakley and T. A. Litowitz, *J. Chem. Phys*., 1974, **60**, 5025.
11 (*a*) A. K. Soper and A. Luzar, *J. Phys. Chem*., 1996, **100**, 1357; (*b*) A. K. Soper and A. Luzar, *J. Chem. Phys*., 1992, **97**, 1320.
12 (*a*) J. E. Bertie and Z. Lan, *Appl. Spectrosc*., 1996, **50**, 1047; (*b*) J. T. Kindt and C. A. Schmuttenmaer, *J. Phys. Chem*., 1996, **100**, 10373.
13 M. Berg and D. A. Vanden Bout, *Acc. Chem. Res*., 1997, **30**, 65.
14 (*a*) D. McMorrow, W. T. Lotshaw and G. Kenney-Wallace, *IEEE J. Quantum Electron*., 1988, **QE–24**, 443; (*b*) S. J. Rosenthal, N. F. Scherer, M. Cho, X. Xie, M. E. Schmidt and G. R. Fleming, in *Ultrafast Phenomena*, ed. J.-L. Martin, A. Migus, G. A. Mourou and A. H. Zewail, Springer, Berlin, 1993; (*c*) R. Righini, *Science*, 1993, **262**, 1386.
15 (*a*) S. Palese, L. Schilling, R. J. D. Miller, P. R. Staver and W. T. Lotshaw, *J. Phys. Chem*., 1994, **98**, 6308; (*b*) E. W. Castner, Jr, Y. J. Chang, Y. C. Chu and G. E. Walrafen, *J. Chem. Phys*., 1995, **102**, 653; (*c*) K. Winkler, J. Lindner, H. Bürsing and P. Vöhringer, *J. Chem. Phys*., 2000, **113**, 4674; (*d*) C. J. Fecko, J. D. Eaves and A. Tokmakoff, *J. Chem. Phys*., 2002, **117**, 1139.
16 (*a*) S. Saito and I. Ohmine, *J. Chem.Phys*., 1997, **106**, 4889; (*b*) I. Ohmine and S. Saito, *Acc. Chem. Res*., 1999, **32**, 741.
17 B. D. Bursulaya and H. J. Kim, *J. Chem. Phys*., 1998, **109**, 4911.
18 A. Perry, H. Ahlborn, B. Space and P. B. Moore, *J. Chem. Phys*., 2003, **118**, 8411.
19 M. A. Ricci, G. Ruocco and M. Sampoli, *Mol. Phys*., 1989, **67**, 19.
20 M. S. Skaf and S. M. Vechi, *J. Chem. Phys*., 2003, **119**, 2181.
21 H. Torii, *Chem. Phys. Lett*., 2003, **353**, 431.
22 B. J. Berne and R. Pecora, *Dynamic Light Scattering*, Dover, Mineola, 2000.
23 S. Mukamel, *Principles of Nonlinear Optical Spectroscopy*, Oxford University Press, New York, 1999.
24 (*a*) L. C. Geiger and B. M. Ladanyi, *J. Chem. Phys*., 1987, **87**, 191; (*b*) L. C. Geiger and B. M. Ladanyi, *Chem. Phys. Lett*., 1989, **159**, 413; (*c*) B. M. Ladanyi, *Chem. Phys. Lett*., 1985, **121**, 351; (*d*) P. A. Madden, in *Ultrafast Phenomena*, ed. D. H. Auston and K. B. Eisenthal, Springer, Berlin, 1985, vol. IV, p. 244; (*e*) T. L. C. Jansen, J. G. Snijders and K. Duppen, *J. Chem. Phys*., 2001, **114**, 10910; (*f*) K. Kiyohara, K. Kamada and K. Ohta, *J. Chem. Phys*., 2000, **112**, 6338; (*g*) H. Stassen, Th. Dorfmüller and B. M. Ladanyi, *J. Chem. Phys*., 1994, **100**, 6318; (*h*) O. Faurskov Nielsen, *Annu. Rep. Prog. Chem., Sect. C*, 1993, **90**, 3.
25 M. J. Frisch, G. W. Trucks, H. B. Schlegel, G. E. Scuseria, M. A. Robb, J. R. Cheeseman, V. G. Zakrzewski, J. A. Montgomery, Jr., R. E. Stratmann, J. C. Burant, S. Dapprich, J. M. Millam, A. D. Daniels, K. N. Kudin, M. C. Strain, O. Farkas, J. Tomasi, V. Barone, M. Cossi, R. Cammi, B. Mennucci, C. Pomelli, C. Adamo, S. Clifford, J. Ochterski, G. A. Petersson, P. Y. Ayala, Q. Cui, K. Morokuma, D. K. Malick, A. D. Rabuck, K. Raghavachari, J. B. Foresman, J. Cioslowski, J. V. Ortiz, A. G. Baboul, B. B. Stefanov, G. Liu, A. Liashenko, P. Piskorz, I. Komaromi, R. Gomperts, R. L. Martin, D. J. Fox, T. Keith, M. A. Al-Laham, C. Y. Peng, A. Nanayakkara, C. Gonzalez, M. Challacombe, P. M. W. Gill, B. G. Johnson, W. Chen, M. W. Wong, J. L. Andres, M. Head-Gordon, E. S. Replogle and J. A. Pople, *GAUSSIAN 98 (Revision A.7)*, Gaussian, Inc., Pittsburgh, PA, 1998.
26 A. V. Gubskaya and P. G. Kusalik, *Mol. Phys*., 2001, **99**, 1107.
27 (*a*) G. Maroulis, *Chem. Phys. Lett*., 1998, **289**, 403; (*b*) G. Maroulis, *J. Chem. Phys*., 2000, **113**, 1813.
28 (*a*) J. Kongsted, A. Osted, K. V. Mikkelsen and O. Christiansen, *J. Chem. Phys*., 2003, **119**, 10519; (*b*) J. Kongsted, A. Osted, K. V. Mikkelsen and O. Christiansen, *J. Chem. Phys*., 2004, **120**, 3787.
29 H. J. C. Berendsen, J. R. Grigera and T. P. Straatsma, *J. Phys. Chem*., 1987, **91**, 6269.
30 (*a*) S. W. de Leeuw, J. M. Perram and E. R. Smith, *Annu. Rev. Phys. Chem*., 1986, **37**, 245; (*b*) S. W. de Leeuw, J. M. Perram and E. R. Smith, *Proc. R. Soc. London, Ser. A*, 1980, **373**, 27; (*c*) S. W. de Leeuw, J. M. Perram and E. R. Smith, *Proc. R. Soc. London, Ser. A*, 1980, **373**, 57.
31 J. P. Ryckaert, G. Ciccotti and H. J. C. Berendsen, *J. Comput. Phys*., 1977, **23**, 327.
32 (*a*) M. P. Allen and D. J. Tildesley, *Computer Simulation of Liquids*, Clarendon, Oxford, 1989; (*b*) R. W. Hockney, *Methods Comput. Phys*., 1970, **9**, 136.
33 P. P. Wiewior, H. Shirota and E. W. Castner Jr, *J. Chem. Phys*., 2002, **116**, 4643.
34 R. Torre, P. Bartolini and R. Righini, *Nature*, 2004, **428**, 296.
35 (*a*) D. M. F. Edwards and P. A. Madden, *Mol. Phys*., 1984, **51**, 1163; (*b*) M. S. Skaf, T. Fonseca and B. M. Ladanyi, *J. Chem. Phys*., 1993, **98**, 8929.
36 B. M. Ladanyi and Y. Q. Liang, *J. Chem. Phys*., 1995, **103**, 6325.
37 M. Cho, M. Du, N. F. Scherer, G. R. Fleming and S. Mukamel, *J. Chem. Phys*., 1993, **99**, 2410.
38 B. M. Ladanyi and S. Klein, *J. Chem. Phys*., 1996, **105**, 1552.
39 Y. J. Chang and E. W. Castner Jr, *J. Chem. Phys*., 1993, **99**, 7289.
40 B. D. Bursulaya and H. J. Kim, *J. Phys. Chem. B*, 1997, **101**, 10994.
41 J. Borysow, M. Moraldi and L. Frommhold, *Mol. Phys*., 1985, **56**, 913.

